materials

MDPI

Article

Effects of V_2O_3 and SiO_2 Contents on the Viscosity and Surface Tension of V_2O_3–FeO–SiO_2–TiO_2–MnO Vanadium Slag

Lian Chen [1,†], Huanran Mao [2,†], Liudong Jiang [1], Qi Cheng [2], Jinhong Zhao [2], Zhiming Yan [2], You Wu [3], Guishang Pei [3,*] and Guibao Qiu [2,*]

[1] Pangang Group Research Institute Co., Ltd., Panzhihua 617000, China; pyychenlian@163.com (L.C.); jiang_liudong@outlook.com (L.J.)
[2] School of Materials Science and Engineering, Chongqing University, Chongqing 400044, China; 202409131236b@stu.cqu.edu.cn (H.M.); 18379639453@163.com (Q.C.); zhaojinhong7895@163.com (J.Z.); yanzhiming@cqu.edu.cn (Z.Y.)
[3] Warwick Manufacturing Group, University of Warwick, Coventry CV4 7AL, UK; you.wu.8@warwick.ac.uk
* Correspondence: guishang.pei@warwick.ac.uk (G.P.); qiuguibao@cqu.edu.cn (G.Q.)
† These authors contributed equally to this work.

Highlights

- SiO_2 raises isothermal viscosity overall while lowering critical temperature.
- Higher V_2O_3 contents raise critical temperature and calculated solid precipitation temperatures.
- SiO_2 generally reduces calculated spinel fractions at a given temperature.
- Surface tension generally rises with V_2O_3 content and falls with SiO_2 content.

Abstract

The viscosity and surface tension of converter vanadium slags influence slag flow and slag–metal separation. In this study, two composition series were designed to investigate the V_2O_3-FeO-SiO_2-TiO_2-MnO vanadium slag system containing 8–24 wt.% V_2O_3 or 8–20 wt.% SiO_2, with constant mass ratios among the remaining components in each series. Viscosity and surface tension were measured using a rotational viscometer and the Du Noüy ring method, respectively. Increasing either V_2O_3 or SiO_2 content generally increased isothermal viscosity and the activation energy for viscous flow. The critical temperature increased from 1725 to 1878 K with increasing V_2O_3 content but decreased from 1874 to 1837 K with increasing SiO_2 content. At 1973 K, surface tension increased overall from 304.46 to 331.37 mN/m in the V_2O_3 series and decreased from 374.34 to 354.97 mN/m in the SiO_2 series. These results provide experimental data on the composition-dependent viscosity, critical temperature, and surface tension of the investigated converter vanadium slags.

Keywords: converter vanadium slag; viscosity; surface tension; thermodynamic calculation

Check for updates

Academic Editor: Srecko Stopic

Received: 27 October 2026
Revised: 12 November 2026
Accepted: 13 November 2026
Published: 15 November 2026

Copyright: © 2026 by the authors. Licensee MDPI, Basel, Switzerland. This article is an open access article distributed under the terms and conditions of the Creative Commons Attribution (CC BY) license.

1. Introduction

Vanadium–titanium magnetite (VTM) is an important vanadium resource [1,2]. In the blast furnace–converter vanadium extraction process, vanadium is reduced and transferred to the hot metal before being oxidized and concentrated in the slag during converter blowing [3–5]. The viscosity, surface tension, and melting characteristics of vanadium slags are important physical properties for evaluating their high-temperature behavior and are fundamental to high-temperature slag fluidity and slag–metal separation. V_2O_3 and SiO_2 are important components of converter vanadium slags. The V_2O_3 content reflects

the degree of vanadium enrichment in the slag, whereas SiO_2 formed by silicon oxidation in the hot metal enters the slag and changes its composition. The heat released by silicon oxidation in vanadium-bearing hot metal also affects the heat balance during blowing. Establishing the relationships between these two components and the high-temperature physical properties of vanadium slags therefore provides a basis for studying vanadium extraction in converters.

Previous studies have shown that the structural role of V_2O_3 in vanadium-bearing slags and its effect on viscosity depend on the slag system. Zhang et al. [6] studied the FeO-SiO_2-V_2O_3 system using molecular dynamics (MD) simulations and Fourier transform infrared spectroscopy. They found that increasing the V_2O_3 content decreased the average Si-O-Si bond angle and the degree of polymerization of the silicate network, indicating that V_2O_3 acts as a network modifier in this system. Yehorov et al. [7] found that viscosity decreased with increasing V_2O_3 content in the V_2O_3–CaO–SiO_2–Al_2O_3–MgO–TiO_2 system at a fixed basicity (CaO/SiO_2 = 1.3). Huang et al. [8] described the vanadium-bearing network structure in the FeO–SiO_2–V_2O_3–TiO_2–Cr_2O_3 system as V-O-V chain units and proposed that these units slightly increased the degree of melt polymerization. Liu et al. [9] found that the viscosity of FeO–SiO_2–V_2O_3–TiO_2 slags increased with increasing V_2O_3 content. These findings indicate that the effects of V_2O_3 on slag structure and viscosity depend on the slag system. Its effects on structure and physical properties require further investigation in vanadium slag systems with compositions close to those encountered in industrial practice.

Surface tension is another important parameter for evaluating the high-temperature physical properties of vanadium-bearing slags. Yehorov et al. [7] found that surface tension decreased with increasing V_2O_3 content in the V_2O_3–CaO–SiO_2–Al_2O_3–MgO–TiO_2 system. According to Levchenko et al. [10] Deryabin et al. reported an increase in the surface tension of FeO–SiO_2–V_2O_3 slags upon addition of V_2O_3. However, these studies examined different slag compositions and reported differing trends. Industrial converter vanadium slags are primarily based on the V_2O_3–FeO–SiO_2–TiO_2–MnO quinary system, for which systematic studies of the effects of changes in individual component contents on surface tension are still lacking.

The critical temperature is an important parameter describing solid–liquid phase transitions and the high-temperature melting behavior of slags. It is governed by slag composition, high-temperature phase equilibria, and solid-phase precipitation behavior. Åström et al. [11] studied synthetic slags based on the CaO–SiO_2–MgO– "FeO" system with compositions close to those of electric arc furnace slags. They found that adding V_2O_3 decreased the formation temperatures of dicalcium silicate and the MgO–FeO solid solution. These studies show that compositional changes can affect solid-phase formation and high-temperature slag flow behavior. Changes in the critical temperature of vanadium slags therefore need to be analyzed in conjunction with phase equilibrium calculations.

This study combines thermodynamic calculations with high-temperature experiments to systematically investigate the effects of V_2O_3 and SiO_2 contents on the calculated liquidus temperature, viscosity, surface tension, and critical temperature of the V_2O_3–FeO–SiO_2–TiO_2–MnO quinary vanadium slag system. The results provide a theoretical basis for optimizing the physical properties and controlling the composition of converter vanadium slags.

2. Materials and Methods

2.1. Sample Preparation

Synthetic slags were prepared in the V_2O_3–FeO–SiO_2–TiO_2–MnO system, with the components selected based on the principal oxide constituents of industrial converter

vanadium slags. This simplified system was used to investigate composition–property relationships among the principal components while reducing the complexity associated with simultaneous variations in minor constituents. Two composition series were designed by varying the V_2O_3 and SiO_2 contents, respectively, while maintaining constant nominal mass ratios among the remaining components within each series. Minor constituents of industrial slags, including Cr_2O_3, MgO, Al_2O_3, CaO, and Na_2O, were not included; therefore, the resulting relationships apply to the designed synthetic compositions and experimental conditions. Table 1 lists the nominal batch compositions calculated from the weighed amounts of the starting materials. No chemical analysis was performed on the slag samples following the high-temperature physical property measurements.

Table 1. Nominal batch compositions of the synthetic vanadium slags (wt.%).

Sample	V_2O_3	FeO	SiO_2	TiO_2	MnO
V-A1	**8.00**	49.36	20.20	12.34	10.10
V-A2	**12.00**	47.22	19.32	11.80	9.66
V-A3	**16.00**	45.07	18.44	11.27	9.22
V-A4	**20.00**	42.93	17.56	10.73	8.78
V-A5	**24.00**	40.78	16.68	10.20	8.34
Si-B1	20.20	49.36	**8.00**	12.34	10.10
Si-B2	19.76	48.29	**10.00**	12.07	9.88
Si-B3	19.32	47.22	**12.00**	11.80	9.66
Si-B4	18.44	45.07	**16.00**	11.27	9.22
Si-B5	17.56	42.93	**20.00**	10.73	8.78

Note: Bold values indicate the nominal contents of the component varied in each series: V_2O_3 in the V-A series and SiO_2 in the Si-B series.

Analytical-grade SiO_2 and TiO_2 (Sinopharm, Shanghai, China) and MnO (Macklin, Shanghai, China) were used in this study, whereas V_2O_3 and FeO were prepared in the laboratory. V_2O_3 was prepared from V_2O_5 powder. The powder was mixed with additions of 2 wt.% maltodextrin and 5 wt.% deionized water, pelletized, and placed in a vertical reduction furnace. After three evacuation–argon backfilling cycles, H_2 was introduced at 400 mL/min. Stepwise reduction was performed at a heating rate of 10 K/min. The pellets were held at 473 K and 673 K for 1 h each to remove moisture and binder, respectively, followed by a 1.5 h hold at 773 K to promote the reduction of V^{5+} to V^{4+}. A final hold at 973 K for 2 h completed the reduction to V^{3+}. The preparation procedure is shown in Figure 1. FeO was prepared by reacting analytical-grade Fe and Fe_3O_4 powders. The powders were mixed at a molar ratio of 1:1, pressed into compacts, and heated in a dual-zone tube furnace at 1373 K for 10 h under high-purity argon (>99.99%). The furnace was then cooled to 873 K, and the samples were transferred rapidly to the cold zone inside the furnace. After cooling to room temperature, the samples were crushed for subsequent use. The X-ray diffraction (XRD; Empyrean, PANalytical, Almelo, The Netherlands) patterns of the laboratory-prepared V_2O_3 and FeO are shown in Figure 2. For each composition listed in Table 1, the raw materials were weighed to a total mass of 180 g and thoroughly mixed. The mixture was then compacted at 36 MPa and loaded into a high-purity molybdenum crucible for high-temperature physical property measurements.

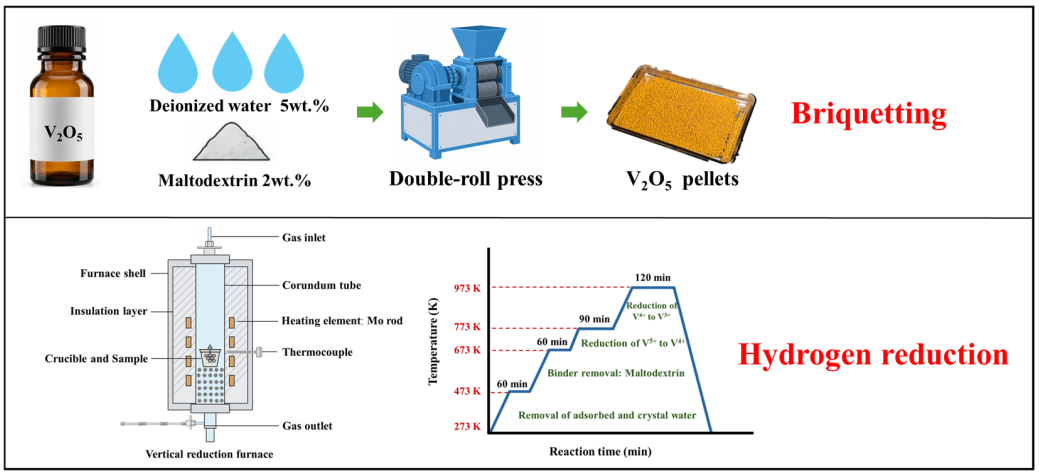


Figure 1. Schematic diagram of the V_2O_3 preparation procedure.

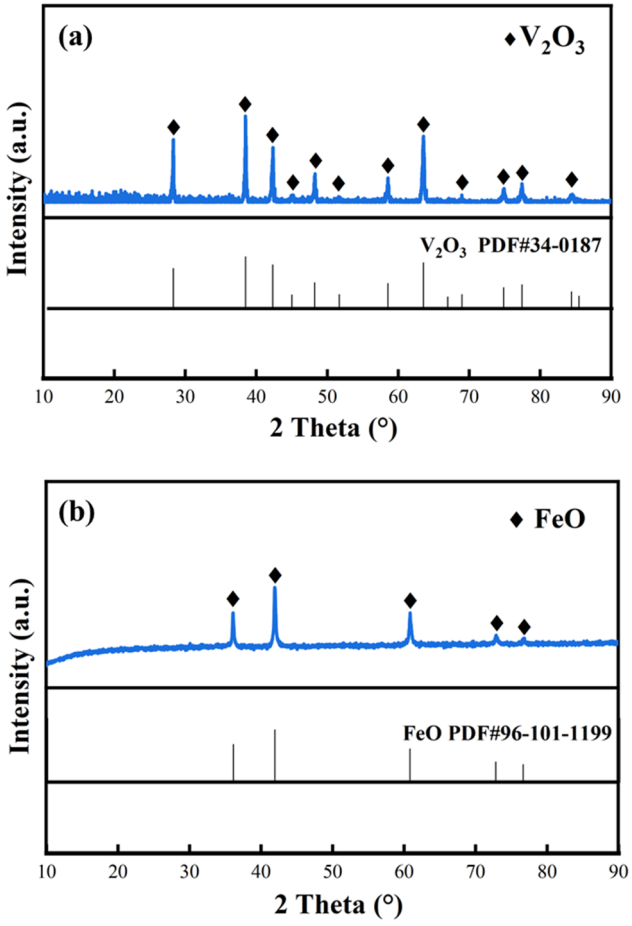


Figure 2. X-ray diffraction (XRD) patterns of the laboratory-prepared (**a**) V_2O_3 and (**b**) FeO samples. The numbers following "PDF#" identify the reference diffraction patterns used for phase identification.

2.2. Thermodynamic Calculations of Phase Evolution

Thermodynamic calculations of phase evolution during slag cooling were performed using the Equilib module of FactSage 8.1 with the FactPS, FToxid, and FTmisc databases. The nominal batch compositions listed in Table 1 were used as the initial inputs. Changes in phases and their mass fractions during cooling from 2073 to 1273 K were calculated using

the Scheil–Gulliver mode at a total pressure of 1 atm. No fixed oxygen partial pressure was imposed; the initial composition was defined by the input oxides and their amounts.

The standard Scheil–Gulliver model assumes complete mixing in the liquid and no diffusion within the solids, with previously precipitated solids no longer re-equilibrating with the remaining liquid. The calculated precipitation sequence and temperatures of individual solid phases, together with the calculated liquidus temperature of each slag, were analyzed to support the interpretation of composition-dependent changes in slag physical properties. The calculation inputs were not adjusted using post-test chemical analyses, and the results were used to examine crystallization trends during cooling for the specified initial compositions.

2.3. Viscosity and Surface Tension Measurements

High-temperature viscosity and surface tension were measured using a high-temperature physical property measurement system developed at Chongqing University [12]. Before testing, the viscosity and surface tension measurement systems were calibrated at 298.15 K using silicone oil and deionized water, respectively. Surface tension was measured using the Du Noüy ring method with a molybdenum ring. High-purity argon (>99.99%) was supplied continuously during the experiments to reduce exposure of the slag samples and molybdenum measurement components to the external oxidizing atmosphere.

2.3.1. Viscosity Measurements

The viscosity of the vanadium slags was measured using a Brookfield LV rotational viscometer (model DV2T; AMETEK Brookfield, Middleboro, MA, USA) equipped with a custom-made molybdenum spindle. The spindle diameter was 13.86 mm. Slag samples V-A4 and V-A5 were heated to 1998 K at a rate of 10 K/min, whereas all other samples were heated to 1973 K at the same rate. All samples were held at their respective maximum heating temperatures for 2 h. Mechanical stirring was performed every 20 min during this period to promote melting and thermal and compositional uniformity. The spindle was then lowered slowly to an immersion depth of 27 mm. Viscosity was recorded after the rotational speed and torque readings had stabilized.

Isothermal viscosity was measured during stepwise cooling at a constant rotational speed of 90 rpm for all slag samples. At each target temperature, the sample was held for 30 min. After stabilization, three viscosity readings were collected from the same slag sample during a single experimental run, and their arithmetic mean was reported. These readings did not represent three independent experiments involving separate sample preparation and heating.

The critical temperature (T_{cr}) was determined from the viscosity–temperature curve obtained during continuous cooling at 2 K/min. The initial rotational speed was 90 rpm and was subsequently adjusted automatically by the measurement system. The experimental data were plotted in Origin 2021 using linear axes, with temperature (K) on the horizontal axis and viscosity (dPa·s) on the vertical axis. In the region where viscosity increased rapidly during cooling, a straight line with a fixed slope of -1 dPa·s·K^{-1} was constructed [13]. Its intercept was adjusted until the line was tangent to the viscosity–temperature curve, and the temperature at the tangency point was defined as the critical temperature in this study.

Isothermal viscosity was obtained from isothermal measurements following stepwise cooling, whereas the critical temperature was determined from viscosity–temperature curves recorded during continuous cooling. The two procedures impose different thermal histories, and differences in holding time and cooling conditions may affect crystallization kinetics and solid fractions. The critical temperature therefore characterizes viscosity variation under the continuous-cooling and rotational-speed protocol specified in this study.

2.3.2. Surface Tension Measurements

The surface tension of the vanadium slags was measured using the Du Noüy ring method [14,15]. The measurement assembly consisted of an electronic balance, a lifting platform, and a molybdenum ring assembly. The balance was mounted on the lifting platform, with a molybdenum rod suspended beneath it. A custom-made molybdenum ring was attached to the lower end of the rod. The mean ring diameter was 17.66 mm. During measurement, the platform moved the balance and the entire ring assembly vertically, while the balance continuously recorded the force during withdrawal. After the viscosity measurements, the slag sample was reheated to 1973 K and held for 30 min. Surface tension was then measured sequentially at 1973, 1923, and 1873 K during stepwise cooling at intervals of 50 K.

For each measurement, the balance and suspended ring were slowly lowered using the lifting platform. Once the ring contacted the slag surface and a distinct change in the balance reading was observed, the ring was lowered further to approximately 2–3 mm below the surface. After the balance reading and slag surface had stabilized, the molybdenum ring was withdrawn vertically at a constant speed of 0.5 mm/s under program control, while the balance continuously recorded the withdrawal force. The maximum force recorded during withdrawal (F_{max}) was used to calculate the surface tension (σ).

Surface tension was calculated from the maximum net force recorded during withdrawal:

$$\sigma = \frac{F_{max}}{2\pi D} \cdot f \quad (1)$$

Here, σ is the surface tension (mN/m), F_{max} is the maximum net withdrawal force after baseline subtraction (mN), and D is the mean molybdenum ring diameter (m). The ring apparatus was calibrated with deionized water at 298.15 K, yielding an empirical correction factor of ($f = 0.78$). This factor was applied consistently to all slag measurements performed with the same ring geometry and withdrawal procedure. The use of this room-temperature factor under high-temperature slag measurement conditions is a source of uncertainty in the reported absolute surface tension values.

For each composition and temperature, three repeated ring-withdrawal measurements were performed on the same slag sample, and the arithmetic mean of the three surface tension values was reported. Error bars represent the standard deviation of the three repeated withdrawal measurements (SD, $n = 3$). These measurements were performed on the same slag sample rather than in three experiments using independently prepared samples.

3. Results and Discussion

3.1. Effects of V_2O_3 Content on Slag Viscosity and Surface Tension

3.1.1. Effect of V_2O_3 Content on Phase Equilibria

The calculated phase fractions during cooling and liquidus temperatures of slags with different V_2O_3 contents are shown in Figure 3. The calculated precipitation temperatures of the solid phases are listed in Table 2. As the V_2O_3 content increased from 8 to 24 wt.%, the calculated liquidus temperature increased from 1464.41 to 2027.81 K, indicating that increasing the V_2O_3 content promoted solid-phase formation at higher temperatures within the investigated composition range.

The predicted primary phase also changed with composition. At 8 wt.% V_2O_3, the primary phase was a Ti-bearing spinel, labeled Ti-SPINB in the figure. At 12 and 16 wt.% V_2O_3, the primary phase changed to a V-bearing spinel, labeled V-SPINB, with calculated precipitation temperatures of 1648.41 and 1846.52 K, respectively. At 20 and 24 wt.% V_2O_3, the primary phase changed to a V_2O_3 solid solution [16]. These calculations indicate that increasing V_2O_3 content raised the liquidus temperature and changed the primary phase

during Scheil–Gulliver cooling, providing a basis for examining the influence of solid-phase precipitation on slag flow behavior in the subsequent measurements.

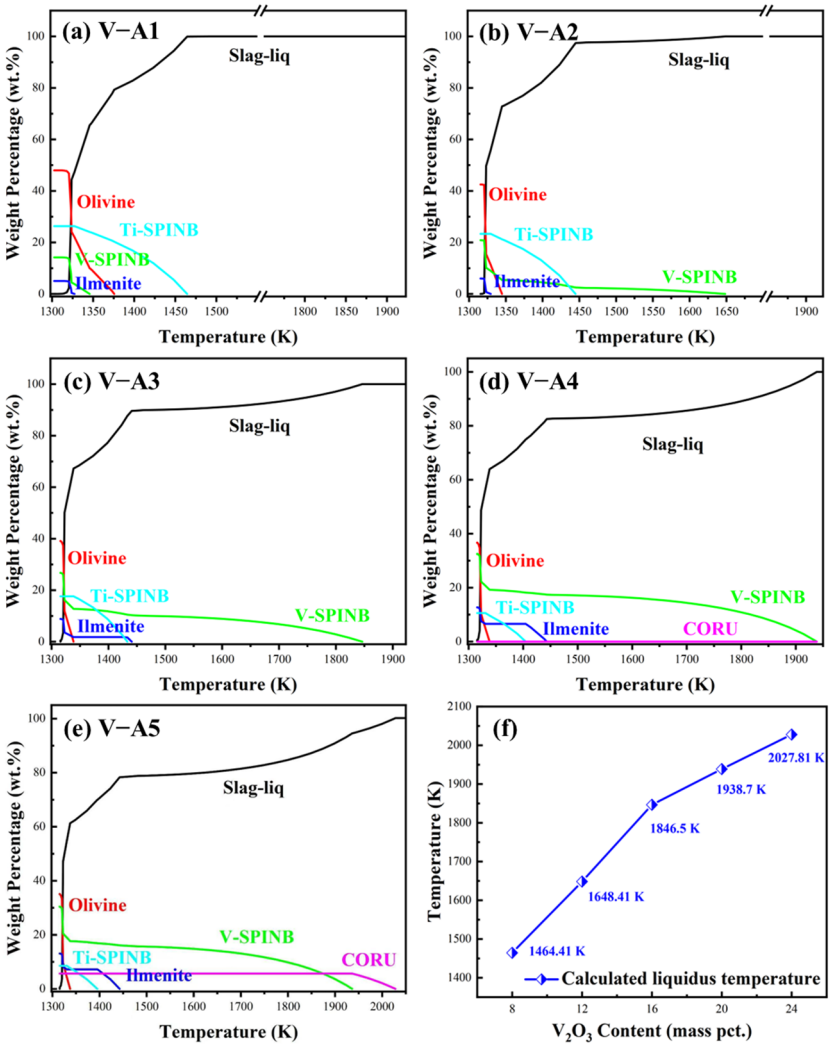


Figure 3. Calculated phase mass fractions during Scheil–Gulliver cooling and liquidus temperatures of slags with different V_2O_3 contents: (**a**) 8, (**b**) 12, (**c**) 16, (**d**) 20, (**e**) 24 wt.% V_2O_3 and (**f**) calculated liquidus temperature as a function of V_2O_3 content. For clarity, the breaks in the temperature axes of panels (**a**,**b**) omit intervals in which the calculated liquid mass fraction remains at 100%.

Table 2. Calculated precipitation temperatures of each phase for slags with varying V_2O_3 contents (K).

Phase	V-A1	V-A2	V-A3	V-A4	V-A5
CORU	—	—	—	1938.7	2027.81
V-SPINB	1345.77	1648.41	1846.52	1938.62	1938.36
Ti-SPINB	1464.41	1444.75	1433.21	1404.40	1398.63
Ilmenite	1327.33	1329.47	1440.85	1443.28	1443.73
Olivine	1375.66	1344.72	1338.56	1338.34	1338.23

3.1.2. Effect of V_2O_3 Content on Viscosity and Activation Energy for Viscous Flow

Figure 4a shows the effect of V_2O_3 content on isothermal slag viscosity at different temperatures. Measurements at 1998 K were performed only for V-A4 and V-A5, consistent with the higher maximum heating temperature used for these samples. For V-A5, the maximum heating temperature of 1998 K was below its calculated liquidus temperature of

2027.81 K. The possible presence of solids was therefore considered when interpreting its viscosity data. The activation energy derived from these data characterizes the temperature dependence of the measured viscosity over the fitted interval and is not assigned specifically to the fully liquid slag. Within the composition range measured at each temperature, isothermal viscosity generally increased with increasing V_2O_3 content. The thermodynamic calculations indicate that slags with higher V_2O_3 contents had higher calculated liquidus temperatures. Small amounts of fine crystals may therefore precipitate within the melt at some measurement temperatures without producing macroscopic changes in the viscosity–temperature curves. Solid particles dispersed and suspended in the melt increase the effective solid volume fraction. According to the Einstein–Roscoe equation, an increase in the effective solid volume fraction increases the apparent viscosity. However, the solid volume fraction, particle size, and particle distribution at the measurement temperatures were not measured directly in this study. The contribution of solid particles to the viscosity changes therefore cannot yet be determined.

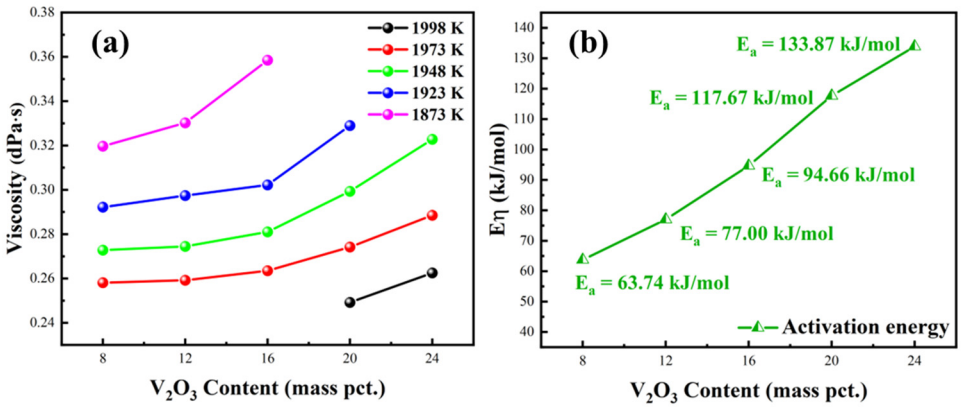


Figure 4. Effect of V_2O_3 content on the properties of vanadium slags: (**a**) isothermal viscosity; (**b**) activation energy for viscous flow. Viscosity data at 1998 K are reported only for V-A4 and V-A5.

Changes in melt structure also affect the viscosity of vanadium slags, although existing interpretations of the structural role of V_2O_3 depend on the slag system. Changes in vanadium-bearing structural units may also influence slag viscosity. V–O–V chain units have been reported in vanadium-bearing slags and can contribute to melt polymerization [8]. Such structural linkages provide a possible contribution to flow resistance in these slags. An increase in viscosity with increasing V_2O_3 content has also been observed in the FeO–SiO_2–V_2O_3–TiO_2 system [9]. Based on these studies, the increase in viscosity with increasing V_2O_3 content may be related to the effects of vanadium-bearing structural units on melt network polymerization. However, this study provides no direct structural characterization evidence, and this interpretation requires verification by Raman spectroscopy, FTIR spectroscopy, or molecular dynamics simulations.

The temperature dependence of viscosity was described using the Arrhenius relationship:

$$\eta = \mathrm{A}\exp\left(\frac{E_\eta}{\mathrm{R}T}\right) \tag{2}$$

Taking the natural logarithm of both sides gives:

$$ln\ \eta = \ln\ \mathrm{A} + \frac{E_\eta}{1000\mathrm{R}} \cdot \frac{1000}{T} \tag{3}$$

where η is the apparent viscosity (dPa·s), A is the pre-exponential factor, E_η is the activation energy for viscous flow (J/mol), R is the gas constant (8.314 $J{\cdot}mol^{-1}{\cdot}K^{-1}$), and T is the absolute temperature (K). Linear regression of ln η against 1000/T was performed using

Origin within the sample-specific temperature intervals. Each temperature point was represented by the arithmetic mean of three viscosity readings. The activation energy and its standard error were calculated from the linear fitting results and converted to kJ/mol for reporting.

The fitting results are shown in Figure 4b. As the V_2O_3 content increased from 8 to 24 wt.%, the activation energy for viscous flow increased from 63.74 to 133.87 kJ/mol. Because some slag samples may contain solids, these activation energies alone cannot establish an increase in the degree of network polymerization of the liquid slag.

3.1.3. Effect of V_2O_3 Content on Critical Temperature

Figure 5 presents the viscosity–temperature curves of slags with different V_2O_3 contents and the critical temperatures determined using the tangent criterion described in Section 2.3.1. As the V_2O_3 content increased from 8 to 24 wt.%, the measured critical temperature increased from 1725 to 1878 K.

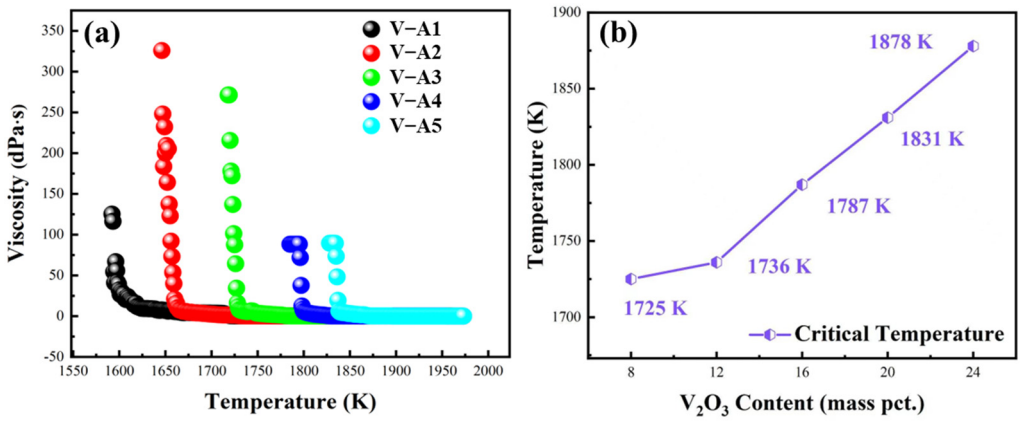


Figure 5. (**a**) Viscosity–temperature curves and (**b**) critical temperatures (T_{cr}) of vanadium slags with different V_2O_3 contents.

The calculations in Figure 3 predict that increasing the V_2O_3 content shifts the onset of solid precipitation to higher temperatures and changes the primary phase from a Ti-bearing spinel to a V-bearing spinel and subsequently to a corundum-type V_2O_3 solid solution. Where solids are present during cooling, they may contribute to the increase in the measured slag viscosity. The predicted phase evolution therefore provides a qualitative basis for interpreting the increase in critical temperature across the V_2O_3 series.

The calculated liquidus temperature describes the predicted onset of solid formation for the nominal batch composition, whereas the critical temperature is obtained from the fixed-slope tangent to the experimental viscosity–temperature curve. For V-A1 and V-A2, the measured critical temperatures of 1725 and 1736 K exceed their calculated liquidus temperatures of 1464.41 and 1648.41 K, respectively. The calculations do not predict solid precipitation at the measured critical temperatures of these two samples and therefore do not support assigning their viscosity transitions to solid precipitation. The quantitative phase predictions are also subject to uncertainty in the thermodynamic description of the multicomponent V-bearing slag system. Accordingly, the calculations are used to interpret composition-dependent crystallization trends, and the critical temperatures are reported as experimental viscosity-based parameters.

3.1.4. Effect of V_2O_3 Content on Surface Tension

Figure 6 shows the effect of V_2O_3 content on slag surface tension at different temperatures. At 1873, 1923, and 1973 K, surface tension generally increased with V_2O_3 content

over the respective measured composition ranges. For a given composition, surface tension generally decreased with increasing temperature.

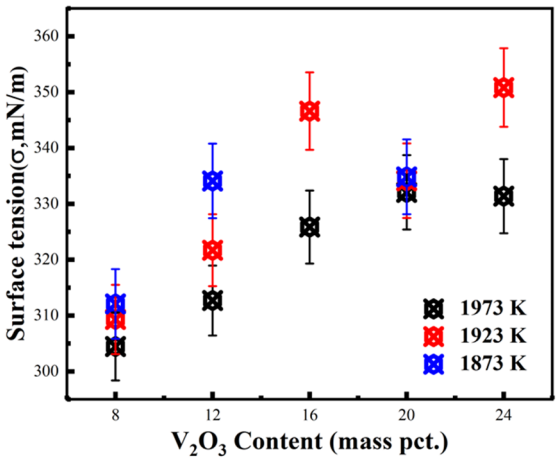


Figure 6. Effect of V_2O_3 content on the surface tension of vanadium slags at different temperatures. Data points represent the arithmetic mean of three repeated ring-withdrawal measurements on the same slag sample at each temperature. Error bars indicate the standard deviation ($n = 3$).

The surface tension of oxide melts depends on their surface composition and ionic structure [17]. In the nominal batch compositions investigated here, increasing the V_2O_3 content was accompanied by corresponding decreases in the mass fractions of SiO_2, FeO, and the other components. SiO_2 lowers the surface tension of FeO-containing silicate melts [18]; its decreasing content can therefore contribute to the observed increase in surface tension. Furthermore, the effects of V_2O_3 and Cr_2O_3 on slag viscosity and surface tension are comparable [19]. Increasing Cr_2O_3 content raises surface tension in CaF_2-CaO-Al_2O_3-based slags and Ti-bearing silicate slags [20,21]. The overall increase in surface tension with V_2O_3 content observed in this study is consistent with these trends.

3.2. Effects of SiO_2 Content on Slag Viscosity and Surface Tension

3.2.1. Effect of SiO_2 Content on Phase Equilibria

The calculated phase mass fractions during cooling and liquidus temperatures of slags with different SiO_2 contents are shown in Figure 7. The calculated precipitation temperatures of the solid phases are listed in Table 3. As the SiO_2 content increased from 8 to 20 wt.%, the calculated liquidus temperature initially decreased, reaching a minimum of 1888.44 K at 10 wt.% SiO_2, and subsequently increased to 1898.10 K at 20 wt.% SiO_2.

Table 3. Calculated precipitation temperatures of each phase for slags with varying SiO_2 contents (K).

Phase	Si-B1	Si-B2	Si-B3	Si-B4	Si-B5
CORU	—	—	—	—	—
V-SPINB	1893.00	1888.44	1889.60	1897.06	1898.10
Ti-SPINB	1545.10	1521.39	1498.71	1455.83	1374.17
Ilmenite	—	1337.83	1338.82	1334.38	1431.63
Olivine	1379.98	1377.79	1369.33	1344.00	1333.61

Throughout the investigated SiO_2 composition range, the calculated primary phase remained a V-bearing spinel, labeled V-SPINB in the figure, and no precipitation of a corundum-type V_2O_3 solid solution was predicted. Under conditions of solid–liquid coexistence, the equilibrium liquid mass fraction at a given temperature generally in-

creased with SiO_2 content, whereas the mass fractions of V-bearing and Ti-bearing spinels decreased correspondingly.

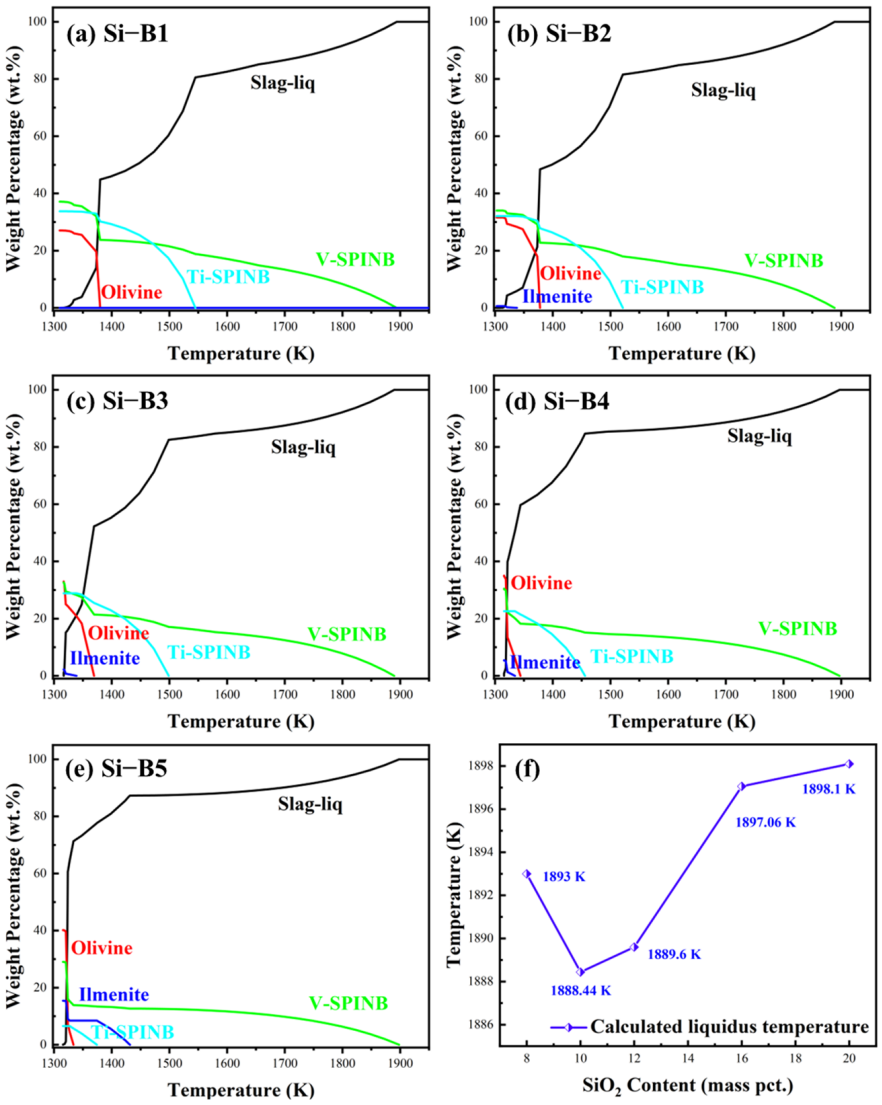


Figure 7. Calculated phase mass fractions during Scheil–Gulliver cooling and liquidus temperatures of slags with different SiO_2 contents: (**a**) 8, (**b**) 10, (**c**) 12, (**d**) 16, and (**e**) 20 wt.% SiO_2 and (**f**) calculated liquidus temperature as a function of SiO_2 content.

3.2.2. Effect of SiO_2 Content on Viscosity and Activation Energy for Viscous Flow

Figure 8 shows the effects of SiO_2 content on slag viscosity and activation energy for viscous flow. Figure 8a indicates that isothermal viscosity generally increased with increasing SiO_2 content. SiO_2 is a typical network former in silicate slags, and the connectivity between $[SiO_4]^{4-}$ tetrahedra is an important factor governing slag viscosity [22,23]. In the nominal batch compositions investigated here, increasing the SiO_2 content was accompanied by corresponding decreases in the mass fractions of basic components, including FeO and MnO. These compositional changes favor greater connectivity between silicate structural units and reduce the depolymerizing effect of basic oxides on the silicate network. The resulting increase in resistance to structural-unit motion explains the overall increase in isothermal viscosity.

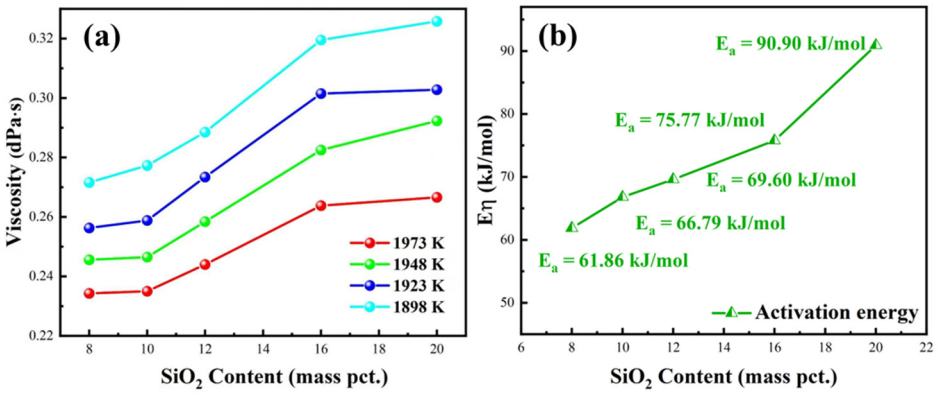


Figure 8. Effect of SiO_2 content on the properties of vanadium slags: (**a**) isothermal viscosity, (**b**) activation energy for viscous flow.

The viscosity–temperature data were fitted using the Arrhenius equation, and the results are shown in Figure 8b. As the SiO_2 content increased from 8 to 20 wt.%, the activation energy for viscous flow increased from 61.86 to 90.90 kJ/mol, indicating greater temperature sensitivity of slag viscosity within the fitted temperature range. The fitting intervals, numbers of distinct temperature points, coefficients of determination (R^2), and activation energies with their standard errors are listed in Table 4.

Table 4. Arrhenius fitting parameters and activation energies for viscous flow of vanadium slags with different compositions.

Sample	Fitting Interval (K)	N	R^2	$E_\eta \pm SE$ (E_η) (kJ/mol)
V-A1	1973–1773	5	0.9823	63.74 ± 4.94
V-A2	1973–1923	3	0.9790	77.00 ± 11.28
V-A3	1973–1923	3	0.9874	94.66 ± 10.69
V-A4	1998–1923	4	0.9910	117.67 ± 7.93
V-A5	1998–1948	3	0.9832	133.87 ± 17.5
Si-B1	1973–1873	5	0.9619	61.86 ± 7.11
Si-B2	1973–1873	5	0.9721	66.79 ± 6.53
Si-B3	1973–1873	5	0.9891	69.60 ± 4.22
Si-B4	1973–1873	5	0.9730	75.77 ± 7.29
Si-B5	1973–1873	5	0.9724	90.90 ± 8.84

Note: N is the number of distinct temperature points included in each fit; R^2 is the coefficient of determination; SE denotes the standard error of a fitted parameter. Each temperature point uses the arithmetic mean of three viscosity readings. E_η is reported as the fitted value ± one standard error.

3.2.3. Effect of SiO_2 Content on Critical Temperature

Figure 9 presents the viscosity–temperature curves of slags with different SiO_2 contents and the critical temperatures determined using the tangent criterion described in Section 2.3.1. At SiO_2 contents of 8, 10, 12, 16, and 20 wt.%, the critical temperatures were 1874, 1866, 1862, 1852, and 1837 K, respectively, decreasing progressively with increasing SiO_2 content.

The thermodynamic calculations in Figure 7 show that the primary phase remained V-bearing spinel as the SiO_2 content increased. Over most of the 1400–1890 K range, the calculated phase mass fractions of V-bearing and Ti-bearing spinels at a given temperature generally decreased, whereas the liquid mass fraction increased correspondingly. According to the Einstein–Roscoe relationship, a lower solid volume fraction reduces the contribution of solid particles to the apparent viscosity of slag. Thus, the reduced spinel precipitation

with increasing SiO_2 content decreases the resistance to slag flow caused by solid particles, thereby contributing to the decrease in critical temperature.

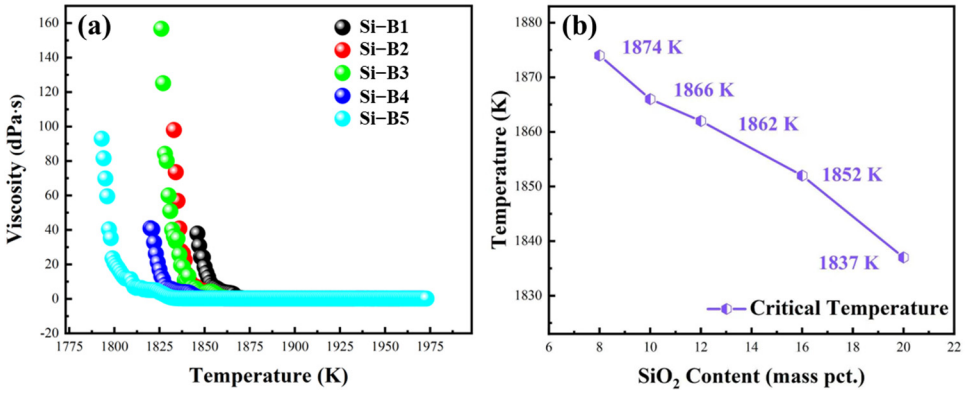


Figure 9. (**a**) Viscosity–temperature curves and (**b**) critical temperatures (T_{cr}) of vanadium slags with different SiO_2 contents.

3.2.4. Effect of SiO_2 Content on Surface Tension

Figure 10 shows the effect of SiO_2 content on slag surface tension at different temperatures. At 1873, 1923, and 1973 K, surface tension generally decreased with increasing SiO_2 content over the respective measured composition ranges. For a given composition, surface tension generally decreased with increasing temperature.

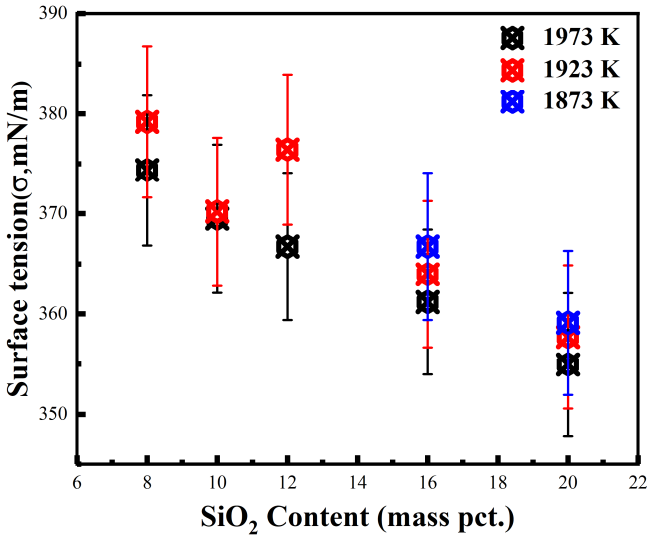


Figure 10. Effect of SiO_2 content on the surface tension of vanadium slags at different temperatures. Data points represent the arithmetic mean of three repeated ring-withdrawal measurements on the same slag sample at each temperature. Error bars indicate the standard deviation ($n = 3$).

SiO_2 is a surface-active component in silicate slags, and increasing its content favors the polymerization of silicate anions and contributes to lowering surface tension [24,25]. The overall decrease in surface tension with increasing SiO_2 content observed in this study is consistent with the reported tendency of SiO_2 to lower the surface tension of silicate melts. Similar decreasing trends have been reported in SiO_2–Al_2O_3–CaO–MgO slags, multicomponent silicate slags containing iron oxides, and FeO–SiO_2 melts [18,24,25].

Some surface tension measurements in Figures 6 and 10 were performed below the calculated liquidus temperatures of the corresponding slags. If solids precipitated under these conditions, they could affect the maximum force recorded during ring withdrawal. Precipitation could also redistribute components between the solid phases and the remaining liquid, causing the liquid composition to deviate from the nominal batch composition and thereby affecting its surface tension. Both effects should be considered when interpreting the reported values at these temperatures.

The composition–property relationships in this study are referenced to the nominal batch compositions. During high-temperature measurements, redox processes involving multivalent elements such as iron and vanadium may alter their oxidation-state distributions. Volatilization losses and interactions between the slags and the molybdenum containers or measurement components may also affect the actual compositions. Although continuous argon protection was employed, these effects were not quantified by post-test chemical analysis. Possible differences between the nominal compositions and those during measurement should therefore be considered a source of uncertainty when interpreting the experimental results and their correspondence with the thermodynamic calculations.

4. Conclusions

The effects of V_2O_3 and SiO_2 contents on the flow-related properties of FeO–SiO_2–V_2O_3–TiO_2–MnO slags were investigated through thermodynamic calculations and high-temperature experiments.

(1) Increasing V_2O_3 content from 8 to 24 wt.% raised the calculated liquidus temperature from 1464.41 to 2027.81 K. The primary phase changed from Ti-bearing spinel to V-bearing spinel and subsequently to a corundum-type V_2O_3 solid solution. SiO_2 content had a smaller effect on the calculated liquidus temperature, which reached a minimum of 1888.44 K at 10 wt.% SiO_2, while V-bearing spinel remained the primary phase.

(2) Isothermal viscosity generally increased with increasing V_2O_3 or SiO_2 content. The Activation energy for viscous flow increased from 63.74 to 133.87 kJ/mol in the V_2O_3 series and from 61.86 to 90.90 kJ/mol in the SiO_2 series, indicating greater temperature sensitivity of viscosity within the fitted temperature ranges.

(3) The measured critical temperature increased from 1725 to 1878 K as the V_2O_3 content increased from 8 to 24 wt.%, and decreased from 1874 to 1837 K as the SiO_2 content increased from 8 to 20 wt.%. The calculations predicted solid precipitation at higher temperatures with increasing V_2O_3 content and generally lower spinel mass fractions with increasing SiO_2 content. These predictions provide qualitative context for interpreting the opposing experimental trends.

(4) Over the investigated temperature and composition ranges, surface tension generally increased with V_2O_3 content and decreased with SiO_2 content. At 1973 K, surface tension increased from 304.46 to 331.37 mN/m in the V_2O_3 series and decreased from 374.34 to 354.97 mN/m in the SiO_2 series. For a given composition, surface tension generally decreased with increasing temperature.

(5) The reported composition–property relationships apply to the nominal batch compositions of the investigated synthetic quinary slags and the laboratory measurement conditions. Minor constituents, fluctuations in chemical and phase composition, and the heterogeneous distribution and aggregation of solid particles in industrial vanadium slags may affect crystallization and flow behavior. Actual compositional changes during high-temperature testing require further assessment through post-test chemical analysis, while industrial application of these results requires validation using actual slags and operating conditions.

Author Contributions: Conceptualization, L.C., H.M. and L.J.; methodology, L.C., H.M. and L.J.; software, L.C. and L.J.; validation, L.J. and H.M.; formal analysis, H.M. and L.J.; investigation, L.C.; resources, L.C. and L.J.; data curation, Q.C. and J.Z.; writing—original draft preparation, L.C., H.M., Q.C., J.Z. and Y.W.; writing—review and editing, G.Q., G.P. and Y.W.; project administration, Z.Y.; funding acquisition, L.C. All authors have read and agreed to the published version of the manuscript.

Funding: This research was funded by the National Natural Science Foundation of China (grant number 52674421) and the Chongqing Young Talents Program (CSTB2025YCJH-KYXM0057).

Data Availability Statement: The original contributions presented in this study are included in the article. Further inquiries can be directed to the corresponding authors.

Acknowledgments: The authors gratefully acknowledge the Analytical and Testing Center of Chongqing University for providing access to the characterization equipment and technical support.

Conflicts of Interest: Lian Chen and Liudong Jiang were employed by the company Pangang Group Research Institute Co., Ltd. The remaining authors declare that the research was conducted in the absence of any commercial or financial relationships that could be construed as a potential conflict of interest.

References

1. Yan, W.; Zhang, B.; Yang, Y.; Li, L.; Li, W. Overview and progress in comprehensive utilization technology of vanadium titanium magnetite resources in China. *Metal. Mine* **2024**, *11*, 70–80.
2. Zhang, L.; Wang, C. Research progress on separation technology and comprehensive utilization of vanadium–titanium magnetite resources. *Conserv. Util. Miner. Resour.* **2023**, *43*, 127–137. [CrossRef]
3. Chang, F.; Zhao, B.; Li, L.; Geng, L.; Zhang, Z. Research status and prospect of vanadium extraction from vanadium titano-magnetite. *Iron Steel Vanadium Titan.* **2018**, *39*, 71–78. [CrossRef]
4. Liu, Z.; Zhang, X.; Ma, D.; Zhao, B.; Wu, W. Theoretical and thermal simulation of vanadium extraction from molten iron in combination blowing converter. *Iron Steel Vanadium Titan.* **2016**, *37*, 1–7. [CrossRef]
5. Liu, R.; Duan, Y.; Liu, X.; Zhang, S.; Guo, H.; Li, Y.; Lü, Q. Current status of vanadium titanomagnetite smelting in China and discussion and prospects for vanadium enrichment in hot metal. *Iron Steel* **2026**, *61*, 1–17.
6. Zhang, Z.; Xie, B.; Zhou, W.; Diao, J.; Li, H.Y. Structural characterization of FeO-SiO_2-V_2O_3 slags using molecular dynamics simulations and FT-IR spectroscopy. *ISIJ Int.* **2016**, *56*, 828–834. [CrossRef]
7. Yehorov, A.; Bachmann, B.; Wei, X.; Bartzsch, G.; Bellé, M.R.; Volkova, O. Thermophysical properties of liquid CaO-SiO_2-Al_2O_3-MgO-TiO_2-V_2O_3 slags. *J. Non-Cryst. Solids* **2022**, *596*, 121865. [CrossRef]
8. Huang, W.J.; Zhao, Y.H.; Yu, S.; Zhang, L.X.; Ye, Z.C.; Wang, N.; Chen, M. Viscosity property and structure analysis of FeO-SiO_2-V_2O-TiO_2-Cr_2O_3 slags. *ISIJ Int.* **2016**, *56*, 594–601. [CrossRef]
9. Liu, S.; Wang, L.; Chou, K.C. Viscosity measurement of FeO-SiO_2-V_2O_3-TiO_2 slags in the temperature range of 1644-1791 K and modelling by using ion-oxygen parameter. *Ironmak. Steelmak.* **2018**, *45*, 641–647. [CrossRef]
10. Levchenko, M.; Kovtun, O.; Patel, S.D.; Endo, R.; Volkova, O. Thermophysical Properties of CaO–SiO_2–Al_2O_3–MgO–TiO_2–FeO_x–V_2O_3 Slag with CaO/SiO_2=1.13 with Different TiO_2 and V_2O_3 Additions. *Steel Res. Int.* **2025**, *96*, 2300848. [CrossRef]
11. Åström, E.; Andersson, A.; Björkman, B.; Björkvall, J. Influence of Vanadium Oxide on the Viscosity Within the CaO–SiO_2–"FeO"–MgO System. *Metall. Mater. Trans. B* **2025**, *56*, 821–832. [CrossRef]
12. Yan, Z. Fundamental Study of the Structure and Properties of Aluminosilicate-Based Blast Furnace Slags. Ph.D. Thesis, Chongqing University, Chongqing, China, 2019.
13. Chang, Z.Y.; Jiao, K.X.; Zhang, J.L.; Ning, X.J.; Liu, Z.Q. Effect of TiO_2 and MnO on Viscosity of Blast Furnace Slag and Thermodynamic Analysis. *ISIJ Int.* **2018**, *58*, 2173–2179. [CrossRef]
14. Du Noüy, P.L. An Interfacial Tensiometer for Universal Use. *J. Gen. Physiol.* **1925**, *7*, 625–631. [CrossRef] [PubMed]
15. Harkins, W.D.; Jordan, H.F. A Method for the Determination of Surface and Interfacial Tension from the Maximum Pull on a Ring. *J. Am. Chem. Soc.* **1930**, *52*, 1751–1772. [CrossRef]
16. Bale, C.W.; Bélisle, E.; Chartrand, P.; Decterov, S.A.; Eriksson, G.; Gheribi, A.E.; Hack, K.; Jung, I.-H.; Kang, Y.-B.; Melançon, J.; et al. FactSage thermochemical software and databases, 2010-2016. *Calphad* **2016**, *54*, 35–53. [CrossRef]
17. Suzuki, M.; Asano, Y.; Ishii, Y. Surface ionic coordination of Al_2O_3-CaO-based molten slag induced by structural relaxation. *J. Am. Ceram. Soc.* **2024**, *107*, 5624–5636. [CrossRef]
18. Kawai, Y.; Mori, K.; Shiraishi, H.; Yamada, N. Surface tension and density of FeO-CaO-SiO_2 melts. *Tetsu-to-Hagané* **1976**, *62*, 53–61. [CrossRef] [PubMed]

19. Shyrokykh, T.; Neubert, L.; Volkova, O.; Sridhar, S. Two potential ways of vanadium extraction from thin film steelmaking slags. *Processes* **2023**, *11*, 1646. [CrossRef]
20. Shi, G.; Zhang, T.; Niu, L.; Dou, Z. Effects of Al_2O_3 and Cr_2O_3 on properties of smelting slag used for the preparation of CuCr alloy by SHS-metallurgy method. *Nonferrous Met. Sci. Eng.* **2019**, *10*, 8–12. [CrossRef]
21. Cui, Y.; Chen, L.; Deng, Y.; Hao, J.; Tian, Z.; Kang, J.; Yang, D.; Qiu, G. Investigation of the Effect of Cr_2O_3 Content on the Surface Tension of Chromium-Containing High-Titanium Blast Furnace Slag. In *Characterization of Minerals, Metals, and Materials 2023*; Springer: Cham, Switzerland, 2023. [CrossRef]
22. Mills, K.C.; Yuan, L.; Jones, R.T. Estimating the physical properties of slags. *J. S. Afr. Inst. Min. Metall.* **2011**, *111*, 649–658.
23. Mills, K.C. The influence of structure on the physico-chemical properties of slags. *ISIJ Int.* **1993**, *33*, 148–155. [CrossRef]
24. Xin, J.; Wang, N.; Chen, M. Surface tension calculation of molten slag in SiO_2-Al_2O_3-CaO-MgO-'FeO'-'Fe_2O_3' Systems based on a statistical modelling approach. *ISIJ Int.* **2020**, *60*, 2306–2315. [CrossRef]
25. Xin, J.; Wang, N.; Chen, M.; Gan, L. Surface tension calculation of molten slag in SiO_2-Al_2O_3-CaO-MgO systems based on a statistical modelling approach. *ISIJ Int.* **2019**, *59*, 759–767. [CrossRef]

Disclaimer/Publisher's Note: The statements, opinions and data contained in all publications are solely those of the individual author(s) and contributor(s) and not of MDPI and/or the editor(s). MDPI and/or the editor(s) disclaim responsibility for any injury to people or property resulting from any ideas, methods, instructions or products referred to in the content.